JOURNAL OF TROPICAL LIFE SCIENCE
2021, Vol. 11, No. 1, 45 – 51
http://dx.doi.org/10.11594/jtls.11.01.06

Research Article

In silico Study Reveals Potential Docking Sites of δ2-isoxazolines Derivates for Inhibiting Russell's Viper PLA_2 Toxin

Tsaniyah Nur Kholilah, Widodo, Nia Kurniawan*

Department of Biology, Faculty of Mathematics and Natural Sciences, Universitas Brawijaya, Malang, 65145 Indonesia

Article history:
Submission July 2019
Revised December 2019
Accepted December 2019

**Corresponding author:*
E-mail: wawan@ub.ac.id

ABSTRACT

Snake venom phospholipase A_2s (svPLA_2s) has been known as the most abundant component and predominant cause of Russell's viper envenomation. Limitation to serum therapy and considerable pharmacological interest led the researcher to synthesized multi-toxic PLA2 inhibitors, δ2-isoxazolines derivate. Although δ2-isoxazolines derivate already proved inhibitor activity in Group II svPLA2 with known IC_{50}, their mechanism of action remains unveiled. Our recent study investigated their inhibitory activity via molecular docking. The virtual screening revealed that the ligand with diverse structures tied to the relatively same active site region. The result sheds light on the significance of His48 and Asp49 as part of the pro-inflammatory eliciting region. ADME analysis was also performed to filter and identify the best potential inhibitor acceptable for human use. This moiety leads to finding a better therapeutic strategy of svPLA2 inhibitors both as an alternative to serum anti-venom treatment.

Keywords: δ2-isoxazolines, Binding site, Daboia russelli, Molecular docking, svPLA2 inhibitors

Introduction

Snakebite envenomation is categorized as one of the less concerned major medical problems in Asia [1]. Venomous snakebites can occur in around 1.8 million people each year worldwide, of which the death rate can reach 125,000 people [2]. There were approximately 1.2 – 2 million envenoming's in Asia and 57,000 – 100,000 deaths due to snakebite [3]. A venomous snake species with widespread distribution and a high degree of envenomation and morbidity is Russell's viper. The bite rate can reach up to 70 per 100.000 people each year, with fatality 2.4 per 100.000 [4].

Phospholipases A2 (PLA2) plays pivotal roles in biological properties in the venom secretory and snakebite envenomation's primary cause [7]. PLA2 constitutes 24% of the whole *Daboia russelli* venom. *In vivo* assay found neurotoxicity and vital organ damages in lung, liver, and kidney with an LD50 value of 0.44 mg/kg body weight of mice [10, 11].

PLA2 encompasses a wide range of pharmacological effects, such as neurotoxicity, hemotoxicity, cytotoxicity, cardiotoxicity, nephrotoxicity, edema, coagulopathy, anti-cancer, and anti-coagulant [6–8]. This enzyme catalyzes the fatty acid hydrolysis from the sn-2 ester bond of membrane glycerolphospholipids. PLA2 also involves in arachidonic acid production from membrane-derived phospholipids. Arachidonic acid is responsible for a few eicosanoid's biosynthesis, such as thromboxane, prostaglandins, and leukotrienes [11]. The increasing level of PLA2 is also related to local and systemic disorders in humans, such as cancer, asthma, cardiovascular, cerebral, and neurodegenerative illnesses [6].

Scientists had discovered many svPLA_2s inhibitors ranging from antibodies and compounds [8], within synthetic and natural products [6]. Due to the limitations of anti-serum therapy and diverse pharmacological effects toxicity in snake envenomation, many scientists have been forcing their efforts to find a novel inhibitor of multi-toxic svPLA_2s [6, 12]. One of them was the δ2-

How to cite:
Kholilah TN, Widodo, Kurniawan N (2021) *In silico* Study Reveals Potential Docking Sites of δ 2-isoxazolines derivates for Inhibiting Russell's Viper PLA_2 Toxin. Journal of Tropical Life Science 11 (1): 45 – 51. doi: 10.11594/jtls.11.01.06.

isoxazolines derivative. Although δ2-isoxazolines derivative had been proved inhibitory activity *in vitro* and *in vivo* as known as IC_{50} in Group II $svPLA_2$ [13], only a few studies in medicinal chemistry and structural biology evolved. Furthermore, since the characteristics of the interaction modes responsible for $svPLA_2$ inhibition have not been investigated so far, we used the molecular docking approach to detect their interaction with VRV-PL-VIIIa toxin.

Material and Methods

The *in silico* study was done using the Window 10 platform of AMD A4-9125 RADEON processor with 4 GB RAM.

Protein target preparation

Protein target *D. russelli's* PLA_2 VRV-PL-VIIIa obtained from Protein Data Bank (PDB; https://www.rcsb.org/) with accession number P59071 [14]. Since there were several crystal structures, further multiple alignments between experiment published crystal structures 1SV3, 3H1X, 1FV0, 1KPM, 1OXL, 2QVD, and 2B17 protein target was executed using "blastp" (http://blast.ncbi.nlm.nih.gov/Blast.cgi). The preferable sequence for the protein target based on the most preserved binding site sequences and mimics wild-type 3D crystal structure of *D. russelli*'s. The alignment displayed using ESPript v.3.0 [15]. The conserved site also validated using CASTp (sts.bioe.uic.edu/castp/) [16]. Before docking, the water and known ligands of the 3D structure removed using PyMol [17].

Ligand molecules preparation

The canonical SMILES of the small molecule of seven δ2-isoxazoline derivatives and co-crystallized inhibitor [18] were mined from PubChem [19] and saved as a single SDF file using ChemMine [20]. To verify whether the *in silico* analysis simulated the previous experimental data, the co-crystal structure inhibitor must be re-docked. The ligands were minimized in energy and ready for docking using Open Babel on PyRx [21].

Molecular docking

Molecular docking executed using AutoDock Vina in PyRx version 0.9.8 [21] to identify the interaction mode between VRV-PL-VIIIa and small molecule inhibitors. The dimensions of the search scape were defined 10 Å x 10 Å x10 Å and confined to the active site of VRV-PL-VIIIa structure His48 and Asp49 [18]. The center coordinate was X:52.7217, Y:36.7356, Z:2.4643. Semi-flexible docking refinement was chosen depending on their possible interaction to demonstrate the ligand capability. In semi-flexible docking, the residue act as the flexible macromolecule receptor, and the small molecules serve as the ligand with a rigid structure. The best binding pose was made based on the lowest binding affinity. Each molecular docking output was then saved as a.pdb file.

Determination of protein-ligand interaction

The interaction between the 3D structure of *D. russelli*'s PLA_2 VRV-PL-VIIIa with each ligand visualized and unified as a single .pdb file using PyMol [17]. Further, the binding of the protein-ligand complex was determined by using PoseView [22] and LigPlot$^+$ v.1.4 [23].

ADME analysis

The absorption, distribution, metabolism, excretion (ADME) properties was calculated using SwissADME (http://www.swissadme.ch) [24]. This website provides computer modeling to calculate physicochemical descriptors, predict ADME parameters, pharmacokinetic properties, drug-likeliness (Lipinski rule of five), and chemical affability of all ligands considered in this study.

Results and Discussions

Two classes of secretory svPLA2 were classified, Group I of family *Elapidae* and *Hydrophiinae* and group II of family *Crotalinae* and *Viperidae*. Class II-A svPLA2 with a residue length of 120–125 amino acids divided into five subgroups at 49th residues: catalytically active Asp49, catalytically inactive or low activity Lys49, Ser49, Asn49, Arg49. The various subgroups identified a broad range of physiological and pathological impacts as their role in prey digestion [6].

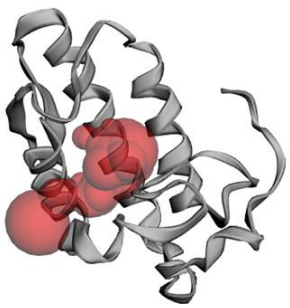

Figure 1. The crystal structure of 1sv3 and predicted pockets on active site cleft

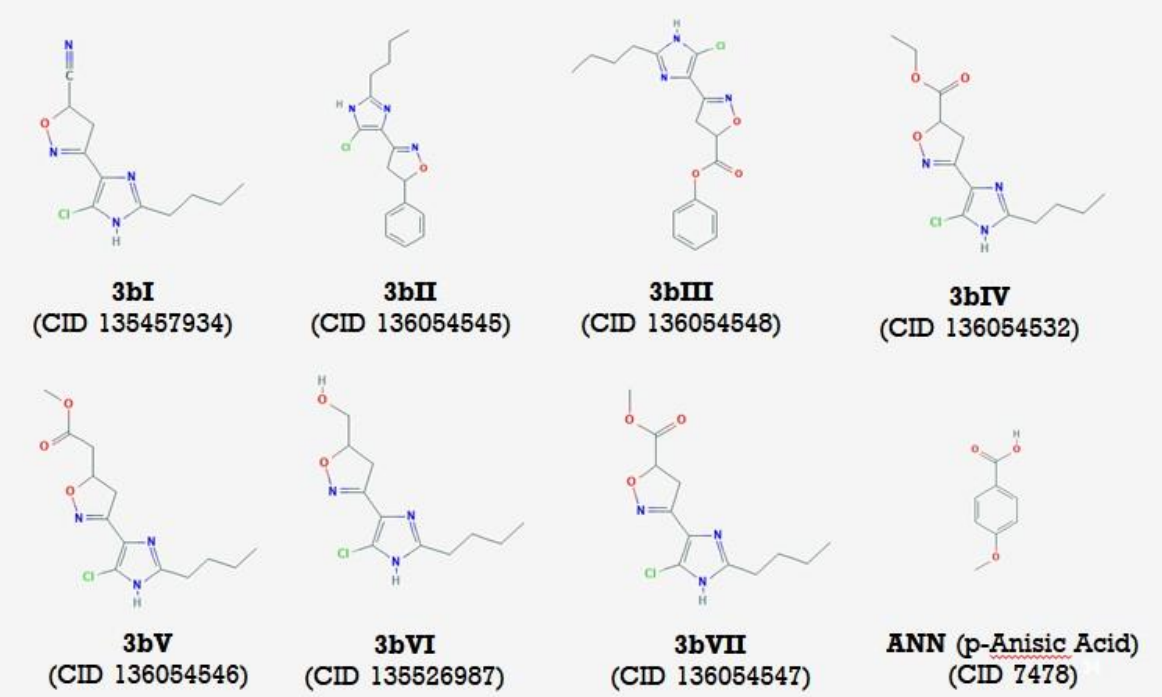

Figure 2. The δ2-isoxazoline derivatives and Anistic acid along with PubChem CID

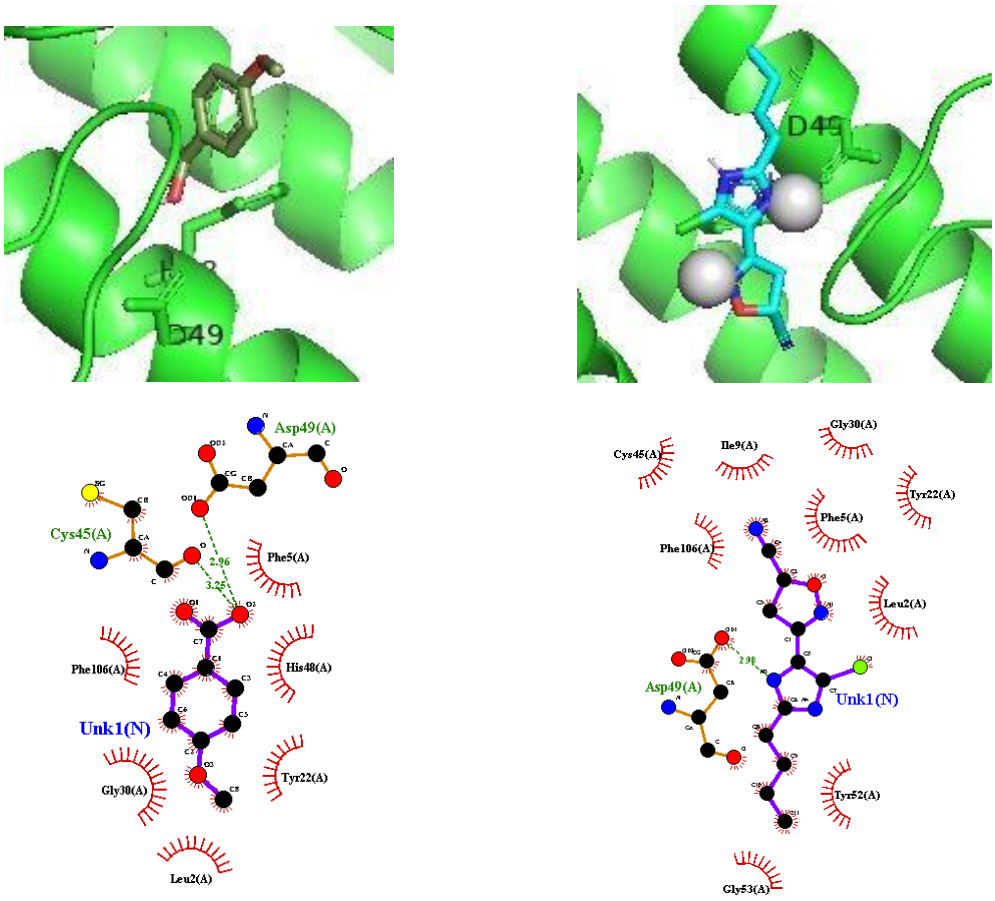

(a) (b)

Figure 3. Interactions protein-ligand binding involving Anisic acid (a) and 3bI of δ2-isoxazoline derivate (b)

Two-thirds of Russell's viper venom proteins composed by svPLA2s provide at least 7 isoforms among the subspecies of *D. russellii* [25]. For this first time, the VRV-PL-VIIIa snake venom structure used to learn the interaction and bonding actions with already identified svPLA2 inhibitors. VRV-PL-VIIIa's multiple sequence alignment between 7 crystal structures showed that sequence identity shares 121 residues indeed with 100 percent query coverage. Since all 3D crystal structures preserved the same sequences, structure 1SV3 was preferred to be the macromolecule receptor, given the highest resolution (1.35 Å). Besides, CASTp confirmed the existence of highly conserved binding sites for Ca^{2+} in residues 27–32 and active site residues for His48 and Asp99, as stated in 1SV3 Uniprot (P59071). These conservative sequences correspond to the pocket, the concavities on the surface of a protein located at the active site cleft (Figure 1).

The crystal structure 1SV3 scaffolded by an α-helix (2–13 residues), an external loop (17–22 residues), a calcium-binding loop (27–32 residues), a second α-helix (39–52 residues), β-turn (66–65 residues) and a third α-helix, a third α-helix (80–98 residues) followed by several η-loop regions finally terminating with the C terminal (Figure 1). Anisic acid (ANN; 4-methoxy benzoic acid) was the co-crystallized inhibitor (Figure 2) [18].

The δ2-isoxazoline derivates were known to inhibit *D. russelli* PLA2 activity with IC_{50} ranged 2.5 – 208 μM. The ancestor, δ2-isoxazoline (PubChem ID: 171639), also reported interfering *D. russelli* PLA2 with IC_{50} 86.2 μM [6]. The δ2-isoxazoline derivative features an ideal filling at the enzyme hydrophobic active site with a butyl substituent. The expansion of ethyl groups increasing the inhibition potential. Based on in vivo study, only compounds 3bI and 3bIV appeared robust inhibition activity of svPLA2. These compounds did not cause edema [13]. However, we employed all seven derivatives in this study to double-check past findings. The structures of the δ2-isoxazoline derivatives are shown in Figure 2.

Molecular docking

Molecular docking demonstrated putative binding modes and protein-ligand site interactions. According to the sequence source, the active site lies on the residue His48 and Asp99, while in the previous study, His48 and Asp49[11, 17]. Residue His48 and Asp49 were part of the sPLA2 domain that including the eliciting pro-inflammatory region. Besides, the Asp99 was part of the region that elicited anti-coagulants. Even so, the *D. russelli* PLA2 enzyme has classified the C-terminal enzyme as Group II Asp49 enzyme[13]. Thus, the molecular docking zones must be limited to the area of Asp49 and His48, so the procedure will be feasible and suitable for screening any other ligands.

In the previous experimental study [18], the carboxylate oxygen atoms of Anisic acid (ANN) bound the water molecule of PLA2 enzyme that interacts with the putative binding residues, Asp 49 and His 48 [18]. It also formed a hydrogen bond with residues from the calcium-binding loop Gly30. Several hydrophobic interactions have been found with residues of α-helix H1 (Leu2, Phe5, Ile9), external loop residues (Ala18, Ile19, Tyr22), and Cys45.

Docking results indicated that all of the small molecules interact with the VRV-PL-VIIIa structure (Figure 3). Ligand ANN formed hydrogen bonds with Asp49 (2.96 Å) and hydrophobic interaction with Leu2, Phe5, Tyr22, Phe106. The contrast of the ANN docking result was the Gly30 and His48 residues interacted as non-hydrogen bonds (Figure 3). Additionally, there were hydrogen bonds with Cys45 (Table 1). Even though not accurately the same interaction, the denoted amino acid residues precisely the same as the previous finding, showing the results of this research mimic the binding mode of the experimental study.

All δ2-isoxazoline derivatives interacted with the critical residues of Asp49 and His48, except for 3bI and 3bII ligands that did not interact with His48. Only small differences in binding affinity between ligand were observed. 3bI displayed the most favorable binding properties compared to other simulated derivatives, similar to the experimental result.

δ2-isoxazoline derivates formed hydrogen bonds with Asp49 residues, except 3bII interacted as hydrophobic. Meanwhile, His48 active site residue has emerged in hydrophobic bonds. The ligand interaction with residues of Asp49 and His48 indicates binding in the pro-inflammatory eliciting area. Besides, several ligands formed hydrogen and hydrophobic bonds with Gly30 to stabilize protein-ligand interactions. Gly30, along with Tyr28 and Gly32, were part of the calcium-binding loop (27–32 residues) via carbonyl oxygen [26]. These discoveries affirmed the capacity of the ligand to cause inhibition activity of VRV-PL- VIIIa. Those small molecules might interfere with the Ca^{2+} catalytic activity, including with PLA2's inflammatory functions [27]. Ca2+ plays

Table 1. Molecular docking result of δ2-isoxazoline derivative against svPLA2 VRV-PL-VIIIa

	Ligand	PubChem ID	IC_{50} (μM)	Binding Affinity	Hydrogen Bond (Å)		Non-Hydrogen Bond
ANN	p-Anisic Acid; 4-methoxy benzoic acid	7478	NA	-5.1	Asp49 Cys45	2.96 3.25	Leu2, Phe5, Tyr22, Gly30, His48, Phe106
3bI	3-(2-Butyl-5-chloro-1H-imidazol- 4-yl)-4,5-dihydro-1,2-oxazole-5- carbonitrile; CHEMBL123168	135457934	96.4	-5.5	Asp49	2.98	Leu2, Phe5, Ile9, Gly30, Cys45, Tyr22, Gly53, Phe106
3bVII	Methyl 3-(2-butyl-5-chloro-1H- imidazol-4-yl)-4,5-dihydro-1,2- oxazole-5-carboxylate; CHEMBL123104	136054547	250	-5.4	Asp49	3.13	Leu2, Phe5, Tyr22, Gly30, Cys45, His48, Tyr52, Lys69
3bVI	[3-(2-Butyl-5-chloro-1H-imidazol- 4-yl)-4,5-dihydro-1,2-oxazol-5- yl]methanol; CHEMBL121517	135526987	151.5	-5.3	Asp49	3.27	Leu2, Phe5, Tyr22, Gly30, Cys45, His48, Tyr52, Phe106
3bIV	Ethyl 3-(2-butyl-5-chloro-1H-im- idazol-4-yl)-4,5-dihydro-1,2-oxa- zole-5-carboxylate; CHEMBL330852	136054532	86.2	-4.9	Asp49 Gly30	2.67 2.74	Leu2, Phe5, Tyr22, Cys29, His48, Tyr52
3bV	Methyl 2-[3-(2-butyl-5-chloro-1H- imidazol-4-yl)-4,5-dihydro-1,2- oxazol-5-yl]acetate; CHEMBL122724	136054546	208.7	-4.5	Asp49 Gly30	2.71 2.81	Leu2, Phe5, Tyr22, Cys29, His48, Tyr52, Lys69
3bII	3-(2-Butyl-5-chloro-1H-imidazol- 4-yl)-5-phenyl-4,5-dihydro-1,2-oxazole; CHEMBL123608	136054545	142	-4.3	-		Leu2, Phe5, Gly30, Asp49, Tyr52
3bIII	Phenyl 3-(2-butyl-5-chloro-1H- imidazol-4-yl)-4,5-dihydro-1,2- oxazole-5-carboxylate; CHEMBL123164	136054548	195	-3.4	Asp49	2.59	Leu2, Phe5, Tyr22, Gly30, Cys45, His48, Tyr52, Phe106

as equilibration in the hemostasis process. Ca^{2+} binding by PLA2 was also related to the hemorrhagic occurrence. This study reinforced the study of VRV PL-VIIIa that targets the pituitary gland and injures the lung leading to hemorrhage [28].

Several hydrophobic interactions that also emerge were residue Leu2 and Phe5 of the α-helix H1 and Tyr22 of the outer loop. It resembled numerous other 3D structures of the sPLA2, in which active sites are highly defined inside a hydrophobic invariant core [29]. Only ligand 3bI found hydrophobic interactions with the region eliciting an anti-coagulant response residue Gly53. The 3bIV ligand, which is also reported to have the best inhibition compared to other δ2-isoxazoline derivates with the least IC50, showed binding affinity -4.9 or not equally with 3bI. The predicted binding affinity could not anticipate the IC_{50} of a ligand against a particular enzyme [26]. Molecular docking only gives a correlation of around 0.5 when compared to experimental data [30]. Hence, it is worth exploring advanced ligand-and-protein interaction through more exact strategies such as end- point free energy through molecular dynamics simulation.

ADME properties

Lead molecules were analyzed based on descriptors that were physically significant and

pharmacologically relevant using SwissADME (Table 2). The analysis also includes Lipinski's five rules for understanding the drug-likeness. All descripttors that are biologically important and pharmaceutically relevant are within the acceptable range for human use. Therefore, 3bI ligand was considered the most potent compound based on water solubility, pharmacokinetics absorption, and drug-likeness.

δ2-isoxazoline derivatives as in silico PLA2 validator

Flooding information on svPLA2 inhibitory activities results in a compromise on the study in silico [8]. To conducting in-silico research on *D. russelli*'s PLA2 while unavailable anti-venom serum chemical structure, δ2-isoxazoline derivatives seem suitable to be the validator. Besides, the δ2-isoxazoline also proven its inhibitory activity on a different subgroup of Group II svPLA2 *D. russelli pulchella* VRV-PL-V that presented His47, Gly48, and Phe5 as interacting residue [6]. These studies coincided that δ2-isoxazoline well conformed the receptor structure on the active site. The known putative binding site of *D. russelli* PLA2 will help to understand the structure and function interaction and in developing other novel and specific inhibitors.

Conclusion

The δ2-isoxazoline derivatives showed the VRV-PL-VIIIa inhibition activity by interacting pro-inflammatory eliciting region on residue Asp49 via hydrogen bonding and His48 via hydrophobic interaction. Among the δ2-isoxazoline derivatives, 3bI possessed the most favorable binding as well as most ideal in the ADME properties. These finding sheds light on the experimental study of alternative serum anti-venom and developing other svPLA2 inhibitors. Further investigation utilizing molecular dynamics simulation is needed for better understanding.

Acknowledgment

T. N. Kholilah thanks to the Ministry of Education and Culture Republic of Indonesia for study financial support toward Beasiswa Unggulan.

References

1. WHO (2016) Guidelines for the management of snakebites. 2nd Edition. India.
2. Slagboom J, Kool J, Harrison RA, Casewell NR (2017) Haemotoxic snake venoms: their functional activity, impact on snakebite victims and pharmaceutical promise. British Journal of Haematology 177(6): 947-959. doi: 10.1111/bjh.14591.
3. Gutiérrez JM, Calvete JJ, Habib AG et al. (2017) Snakebite envenoming. Nature reviews Disease Primers 3 (1): 1-21.
4. Roly ZY, Hakim MA, Zahan AS et al. (2015) ISOB: A Database of Indigenous Snake Species of Bangladesh with respective known venom composition. Bioinformation 11 (2): 107.
5. Berling I, Isbister GK (2015) Hematologic effects and complications of snake envenoming. Transfusion medicine Reviews 29 (2): 82 – 89. doi: 10.1016/j.tmrv.2014.09.005.
6. Sivaramakrishnan V, Ilamathi M, Ghosh KS et al. (2016) Virtual analysis of structurally diverse synthetic analogs as inhibitors of snake venom secretory phospholipase A2. Journal of Molecular Recognition 29 (1): 22-32. doi: 10.1002/jmr.2492.
7. Marcussi S, Sant'Ana CD, Oliveira CZ et al. (2007) Snake venom phospholipase A2 inhibitors: medicinal chemistry and therapeutic potential. Current Topics in Medicinal Chemistry 7 (8): 743-756. doi: 10.2174/156802607780487614.
8. Ojeda PG, Ramírez D, Alzate-Morales J et al. (2018) Computational studies of snake venom toxins. Toxins 10 (1): 8. doi: 10.3390/toxins10010008.
9. Tan KY, Tan NH, Tan CH (2018) Venom proteomics and antivenom neutralization for the Chinese eastern Russell's viper, *Daboia siamensis* from Guangxi and Taiwan. Scientific Reports 8 (1): 1-14. doi: 10.1038/s41598-018-25955-y.
10. Ghag-Sawant M, More TV, Samant LS, Chowdhary AS (2016) Study of neutralization of enzymatic activity of *Daboia russelii* venom by various plant extracts and their combinations using *in vitro* methods. International Journal of Pharmaceutical Sciences and Research 7(6): 2531. doi: 10.13040/IJPSR.0975-8232.7(6)2531-36.
11. Sakthivel G, Dey A, Nongalleima K et al. (2013) In vitro and in vivo evaluation of polyherbal formulation against Russell's viper and cobra venom and screening of bioactive components by docking studies. Evidence-Based Complementary and Alternative Medicine 2013. doi: 10.1155/2013/781216.
12. Dhananjaya BL, Zameer F, Girish KSD, Souza CJ (2011) Anti-venom potential of aqueous extract of stem bark of *Mangifera indica* L. against Daboia russellii (Russell's viper) venom.
13. Basappa, Kumar MS, Swamy SN et al. (2004) Novel δ2-isoxazolines as group II phospholipase A2 inhibitors. Bioorganic Medicinal Chemistry Letters 14 (14): 3679-3681.doi: 10.1016/j.bmcl.2004.05.012.
14. Tsai IH, Lu PJ, Su JC (1996) Two types of Russell's viper revealed by variation in phospholipases A2 from venom of the subspecies. Toxicon 34(1): 99-109.
15. Robert X, Gouet P (2014) Deciphering key features in protein structures with the new ENDscript server. Nucleic Acids Research 42 (W1): W320-W324. doi: 10.1093/nar/gku316.
16. Tian W, Chen C, Lei X et al. (2018) CASTp 3.0: computed atlas of surface topography of proteins. Nucleic Acids Research 46 (W1): W363-W367. doi: 10.1093/nar/gky473.
17. DeLano WL (2002) Pymol: An open-source molecular graphics tool. CCP4 Newsletter on Protein Crystallography 40 (1): 82-92.
18. Singh N, Jabeen T, Pal A et al. (2006) Crystal structures

of the complexes of a group IIA phospholipase A2 with two natural anti-inflammatory agents, anisic acid, and atropine reveal a similar mode of binding. Proteins: Structure, Function, and Bioinformatics 64 (1): 89-100. doi: 10.1002/prot.

19. Kim S, Chen J, Cheng T, Gindulyte A et al. (2019) PubChem 2019 update: improved access to chemical data. Nucleic acids research 47(D1): D1102-D1109. doi: 10.1093/nar/gky1033.
20. Backman TW, Cao Y, Girke T (2011) ChemMine tools: an online service for analyzing and clustering small molecules. Nucleic acids research 39 (suppl 2): W486-W491. doi: 10.1093/nar/gkr320.
21. Trott O, Olson AJ (2010) AutoDock Vina: improving the speed and accuracy of docking with a new scoring function, efficient optimization, and multithreading. Journal of Computational Chemistry 31 (2): 455-461. doi: 10.1002/jcc.21334.
22. Stierand K, Rarey M (2010) Drawing the PDB: protein− ligand complexes in two dimensions. ACS Medicinal Chemistry Letters 1 (9): 540-545. doi: 10.1021/ml100164p.
23. Laskowski RA, Swindells MB (2011) LigPlot+: multiple ligand–protein interaction diagrams for drug discovery.
24. Daina A, Michielin O, Zoete V (2017) SwissADME: a free web tool to evaluate pharmacokinetics, drug-likeness and medicinal chemistry friendliness of small molecules. Scientific Reports 7: 42717. doi: 10.1038/srep42717.
25. Deepa V, Sreekumar S, Biju C (2018) *In silico* validation of anti-russell's viper venom activity in *Phyllanthus emblica* L. and *Tamarindus indica* L. International Journal of Pharmaceutical Sciences and Drug Research 10 (4): 217 – 226. doi: 10.25004/IJPSDR.2018.100403.
26. Apweiler R, Bairoch A, Wu CH et al. (2004) UniProt: the universal protein knowledgebase. Nucleic Acids Research 32 (suppl_1): D115 - D119. doi: 10.1093/nar/gkh131.
27. Mahmud S, Parves MR, Riza YM et al. (2020) Exploring the potent inhibitors and binding modes of phospholipase A2 through *in silico* investigation. Journal of Biomolecular Structure and Dynamics 38 (14): 4221-4231. doi: 10.1080/07391102.2019.1680440.
28. Kumar JR, Basavarajappa BS, Vishwanath BS, Gowda TV (2015) Biochemical and pharmacological characterization of three toxic phospholipase A2s from *Daboia russelii* snake venom. Comparative Biochemistry and Physiology Part C: Toxicology Pharmacology 168: 28-38. doi: 10.1016/j.cbpc.2014.11.005.
29. Dennis EA, Cao J, Hsu YH et al. (2011) Phospholipase A2 enzymes: physical structure, biological function, disease implication, chemical inhibition, and therapeutic intervention. Chemical Reviews 111 (10): 6130-6185.
30. Cheng T, Li X, Li Y et al. (2009) Comparative assessment of scoring functions on a diverse test set. Journal of chemical information and modeling 49 (4): 1079-1093.

This page is intentionally left blank.